How to cite: *Angew. Chem. Int. Ed.* **2023,** *62,* e202305296
doi.org/10.1002/anie.202305296

C-H Activation

C–H Activation of Unbiased C(sp^3)–H Bonds: Gold(I)-Catalyzed Cycloisomerization of 1-Bromoalkynes**

*Rubén Miguélez, Nina Semleit, Carlos Rodríguez-Arias, Pavel Mykhailiuk, José M. González, Gebhard Haberhauer, and Pablo Barrio**

Dedicated to the people of Ukraine

Abstract: Selective functionalization of non-activated C(sp^3)–H bonds is a major challenge in chemistry, so functional groups are often used to enhance reactivity. Here, we present a gold(I)-catalyzed C(sp^3)–H activation of 1-bromoalkynes without any sort of electronic, or conformational bias. The reaction proceeds regiospecifically and stereospecifically to the corresponding bromocyclopentene derivatives. The latter can be readily modified, comprising an excellent library of diverse 3D scaffolds for medicinal chemistry. In addition, a mechanistic study has shown that the reaction proceeds via a so far unknown mechanism: a concerted [1,5]-H shift / C–C bond formation involving a gold-stabilized vinyl-cation-like transition state.

Introduction

Arguably, the selective activation of a non-activated C–H bond is regarded as one of the ultimate reactivities pursued by organic chemists.[1] Among other reasons, this is due to the prevalence of C–H bonds in organic molecules and their similar reactivity, making selectivity a major challenge. In addition, the C–H bonds in aliphatic chains are intrinsically quite inert (bond dissociation energy, BDE 96.5–105 kcal mol^{-1}). Hence, their functionalization requires energetic reaction conditions, resulting in a lack of selectivity. Despite these challenges, several reactions of this kind are well-known. Most of these C–H activation reactions rely on the use of a biased substrate, containing either an activated C–H bond (electronically or conformationally favored) or a directing group, to achieve selectivity.[2,3] The use of chemical reactions that show intrinsic selectivity for the activation of a given C–H bond through an intramolecular mechanism represents an interesting alternative. Furthermore, such intramolecular processes pose the added value of generating a cycle and, hence, on the one hand increasing molecular complexity and, on the other, diminishing the conformational flexibility. Both features are crucial in modern drug discovery.[4,5] In recent years, the deeply rooted preference of certain radicals to undergo [1,5]-hydrogen abstraction has received renewed interest, and several transformations have been reported.[6] This radical approach implies the loss of stereochemical information when the cyclization takes place at a stereocenter (Figure 1A).[7] Similarly, [1,5]-hydride shift processes on cationic intermediates afford planar carbocations and, hence, result in racemic products.[8] Nevertheless, some recent reports have described concerted pathways involving cationic species in which the breaking of the C–H bond occurs concomitantly with the formation of the C–C bond, thus avoiding racemization (Figure 1B).[9,10] In addition to radicals and carbocations, other high-energy intermediates such as carbenes and vinylidenes show an intrinsic preference to react with a C–H placed at the δ-position.[11,12] Hence, [1,5]-C–H insertions of carbene and vinylidene intermediates have commonly been used in the synthesis of 5-membered carbocyclic rings.[13,14] In this context, González, and Zhang have developed gold-catalyzed 5-membered ring formation reactions,[15,16] with the participation of gold-vinylidene intermediates.[17] The latter conceptualized a reaction setup that allowed to access the desired gold-vinylidene intermediate from the corresponding (trimethylsilyl)ynones by treating the gold-acetylide intermediate with a suitable source of electrophilic bromine (Figure 1C).[16] It might seem that the formation of 5-membered rings through the C–H insertion of a gold-carbene(vinylidene) intermediate is already an

[*] R. Miguélez, C. Rodríguez-Arias, Prof. Dr. J. M. González, Dr. P. Barrio
Departamento de química Orgánica e Inorgánica, Universidad de Oviedo
Julian Clavería 8, 33006 Oviedo (Spain)
E-mail: barriopablo@uniovi.es
N. Semleit, Prof. Dr. G. Haberhauer
Institut für Organische Chemie, Universität Duisburg-Essen
Universitätsstraße 7, 45117 Essen (Germany)
Dr. P. Mykhailiuk
Enamine Ltd.
Chervonotkatska 78, 02094 Kyiv (Ukraine)
and
Chemistry Department, Taras Shevchenko National University of Kyiv
Volodymyrska 64, 01601 Kyiv (Ukraine)

[**] A previous version of this manuscript has been deposited on a preprint server (https://doi.org/10.26434/chemrxiv-2022-9twlq-v4).

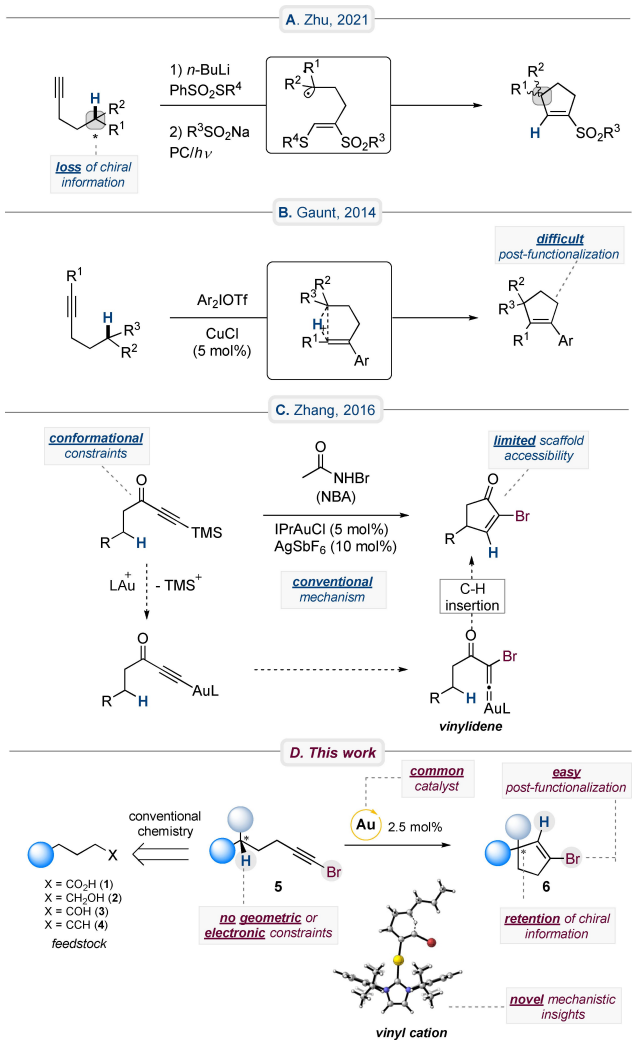

Figure 1. State-of-the-art vs this work.

achieved goal. In summary, all previously published [Au]-catalyzed methods require activation of the triple bond (e.g., by carbonyl or aromatic groups) or of the C(sp^3) center (e.g., by aromatic or cyclopropyl rings).[15,16,18b,c]

Herein, we describe the intramolecular [1,5]-C–H cyclization of a 1-bromoalkyne precursor using a gold(I)-catalyzed insertion into a non-activated C(sp^3)–H bond without any electronic, geometric, or conformational bias (Figure 1D).[19] Some key features of this new transformation are the following: 1) the C(sp^3)–H bond that undergoes activation is truly non-activated (no need for electronic or conformational bias or directing groups); 2) the starting materials are readily available; 3) the reaction conditions are extremely simple (1-bromoalkyne and a common gold(I) source in dicholormethane (DCM) at 80 °C, 2 hours); 4) for the case of the reaction taking place at a stereocenter, the stereochemistry is preserved; 5) the presence of a C(sp^2)–Br bond in the final products makes them extremely useful building blocks and, finally 6) an experimental mechanistic study supported by density functional theory DFT calculations has shown a gold-stabilized vinylcation-like transition state (TS), related to those reported by Gaunt and Nelson.[9,10] It is worth noting that such a reaction pathway has never been observed in gold catalysis.

Hence, the strategy disclosed herein offers valuable new features resulting in a differentiated addition to the synthetic toolbox. The required 1-bromoalkynes (**5**) are readily available from abundant and cheap starting materials such as carboxylic acids (**1**), alcohols (**2**), aldehydes (**3**), or terminal alkynes (**4**) (Figure 2A), through short and manageable reaction sequences.

Results and Discussion

Optimization

As a part of our interest in the chemistry of 1-haloalkynes under gold catalysis and considering that recent reports in this field have focused on aryl-substituted alkynes,[20] our study started with a fundamental question. What is the fate of an aliphatic 1-haloalkyne under gold(I) catalysis in the absence of a reactive counterpart? To answer this question, we carried out a series of experiments using several aliphatic haloalkynes and gold(I) pre-catalysts under several reaction conditions (see Supporting Information, Table S1 for full details). To our delight, we observed that treatment of 1-bromooct-1-yne (**5a**) with a commonly used gold(I) pre-catalyst ([IPrAu(NCMe)][SbF_6]) in 1,2-dichloroethane (DCE) at 65 °C afforded, after 1 hour, 1-bromocyclopentene **6a** in a modest 26 % yield (Table 1). A short optimization of the reaction conditions allowed us to obtain the desired product in an improved 64 % yield just by raising the reaction temperature to 80 °C, changing the solvent to DCM, and increasing the reaction time to 2 hours (Table 1). Unfortunately, the formation of small amounts of a by-product **6a′** (Table 1) and traces of the bromomethyl ketone **6a″** arising from hydration with adventitious water could not be avoided (Table 1).

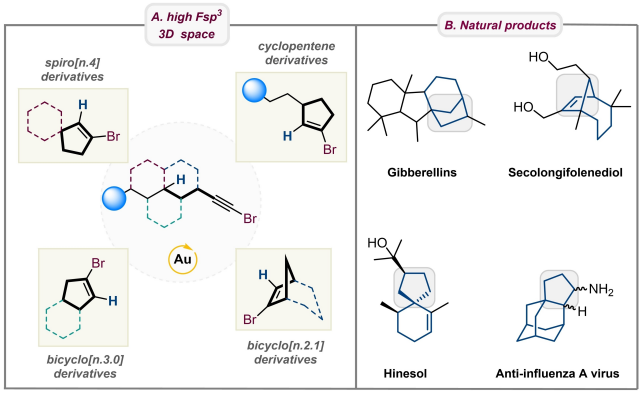

Figure 2. Scaffold accessibility.

Table 1: Optimization.

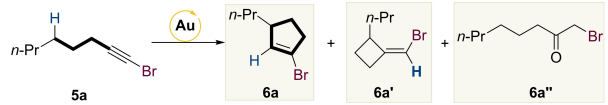

5a 6a 6a' 6a''

10-15 % 5-10%

Entry	Au	Yield
1	[IPrAu(NCMe)][SbF_6] (2.5 mol%), DCE, 65 °C, 8h	26%
2	[IPrAu(NCMe)][SbF_6] (2.5 mol%), DCE, 80 °C, 1h	38%
3	[IPrAu(NCMe)]NTf_2 (2.5 mol%), DCE, 80 °C, 1h	5%
4	[JohnphosAu(NCMe)][SbF_6] (2.5 mol%), DCE, 80 °C, 1h	11%
5	[IPrAu(NCMe)][SbF_6] (2.5 mol%), DCE, 80 °C, 2h	58%
6	[IPrAu(NCMe)][SbF_6] (2.5 mol%), DCM, 80 °C, 2h	64%
7	[IPrAu(NCMe)][SbF_6] (2.5 mol%), DCM, 80 °C, 4Å MS 2h	0%

Scope and limitations

With the optimized conditions in our hands, we examined the new transformation concerning its scope and limitations (Scheme 1). It readily became apparent that alkyl chains of several lengths were tolerated affording the desired products in comparable yields (Scheme 1, linear substrates, **6a–e**). Then, other structural features were considered, mainly the functional group compatibility and the kind of skeletons that can be achieved. Hence, 1-bromoalkynes bearing representative functional groups (protected alcohols, halogens, unsaturated groups, nitrogenated functionalities) in the side chain were synthesized and submitted to the optimized gold-catalyzed reaction conditions. Unfortunately, none of them worked, achieving unreacted starting material as the only recognizable species in the crude nuclear magnetic resonance NMR spectra (Scheme 1, unsuccessful substrates). We hypothesized that the proximity of these polar, non-innocent functional groups may hamper the search for transformation through undesired side reaction pathways involving nucleophilic additions to the activated alkyne and/or catalyst deactivation. Next, we synthesized a second set of functionalized 1-bromoalkynes, this time bearing the functionality at a distal position. First, we selected some of the most common protective groups for alcohols: benzyl (Bn), acetate (Ac), tert-bytyldimethylsilyl (TBS), and methoxymethyl (MOM). From these four substrates, only the acetyl-protected one worked (Scheme 1, remote functional group, **6f**). We reasoned that the diminished nucleophilicity of the ester oxygen as compared to the ether, acetal, and silyl ether functionalities was the key to its success. To challenge this hypothesis, we selected other functional groups that would diminish the nucleophilicity of the oxygen atom attached to the main chain either by conjugation (carbonate and aryl ether) or by increasing the steric bulk (triisopropylsilyl (TIPS) (Scheme 1, remote functional group). As expected, the carbonate group behaved similarly to the acetate, affording product **6g** in good yield. The less efficient conjugation effect of the aryl ether as compared to the carbonyl group resulted in a somewhat lower yield (Scheme 1, remote functional group, **6h**). Finally, even if the chemical yield obtained with the more sterically hindered OTIPS derivative was only fair, it serves as a proof-of-concept (Scheme 1, remote functional group, **6i**). We then used other 1-bromoalkynes bearing poorly nucleophilic functionalities, such as Br, trifluoromethanesulfonate (OTf), phtalimide (NPhTh), an olefin, or a CF_2H at a remote position; all of them worked successfully (Scheme 1, remote functional group, **6j–n**).

Perhaps more interesting than the functional group compatibility was the study of the structural complexity affordable by using this methodology (Scheme 1, cyclic substrates, see the structure of the starting materials and products for the color code). In addition to linear alkynes (black line), the introduction of a cycle separated from the bromoalkyne unit by tethers of different lengths allows a priori access to several kinds of bicyclic structures: directly attached to the ring→bridged bicycle (blue line), one carbon tether→fused bicycle (green line); two carbon tether→spirobicycle (maroon line) (Scheme 1).

According to modern trends in medicinal chemistry, the generation of molecular diversity and complexity is key to the discovery of new action modes.[4,21a] Moreover, all these scaffolds would benefit from a very high C(sp^3) fraction (Fsp^3), meaning the fraction of sp^3 carbon atoms of the total number of carbon atoms (number of Csp^3 / total number of C atoms), another advantageous feature in drug candidates.[21b] This method allowed us to successfully synthesize most of these bicyclic frameworks, although we observed certain limitations. Regarding bridged bicycles, the original cycle in the substrate must be 6- or 7-membered (Scheme 1, cyclic substrates, **6o,p**). Smaller cycles do not react, while bigger ones give rise to mixtures (Scheme 1, unsuccessful substrates). Concerning fused bicycles a similar scenario operates. In this case, 4- and 5-membered rings in the parent bromoalkyne work successfully (Scheme 1, cyclic substrates, **6q,r**), whereas increased ring sizes afford diastereomeric mixtures (Scheme 1, cyclic substrates, **6s,t**). Finally, the formation of spirocycles seems to be the bicyclic system this methodology is best suited for, tolerating 4-, 5-, 6- and 7-membered carbocycles in the substrate (Scheme 1, cyclic substrates, **6u–y**).[22] In contrast, the cyclopropane ring does not participate in the cyclization towards either fused bicycles or spirocycles (Scheme 1, unsuccessful substrates).

Finally, this methodology was challenged by several natural products (NP) derived and complex molecular architectures (Scheme 1, NP-derived and complex substrates). Hence, a 1-bromoalkyne derived from oleic acid in three trivial steps afforded the corresponding product **6z**. The versatility of our synthetic route (see Supporting Information) allowed us to prepare two different derivatives from citronellal. These substrates were used as a probe to test the stereochemical outcome of our reaction. Most importantly, the absolute stereochemistry is preserved when the C–H that participates in the cyclization belongs to a stereocenter (**6aa**). On the other hand, when the reactive CH is adjacent to a stereocenter a mixture of diastereoisomers is formed (**6ab**). Moreover, the 1-bromoalkyne subunit may be attached to a biomolecule through esterification (among other possible ways), and then submitted to

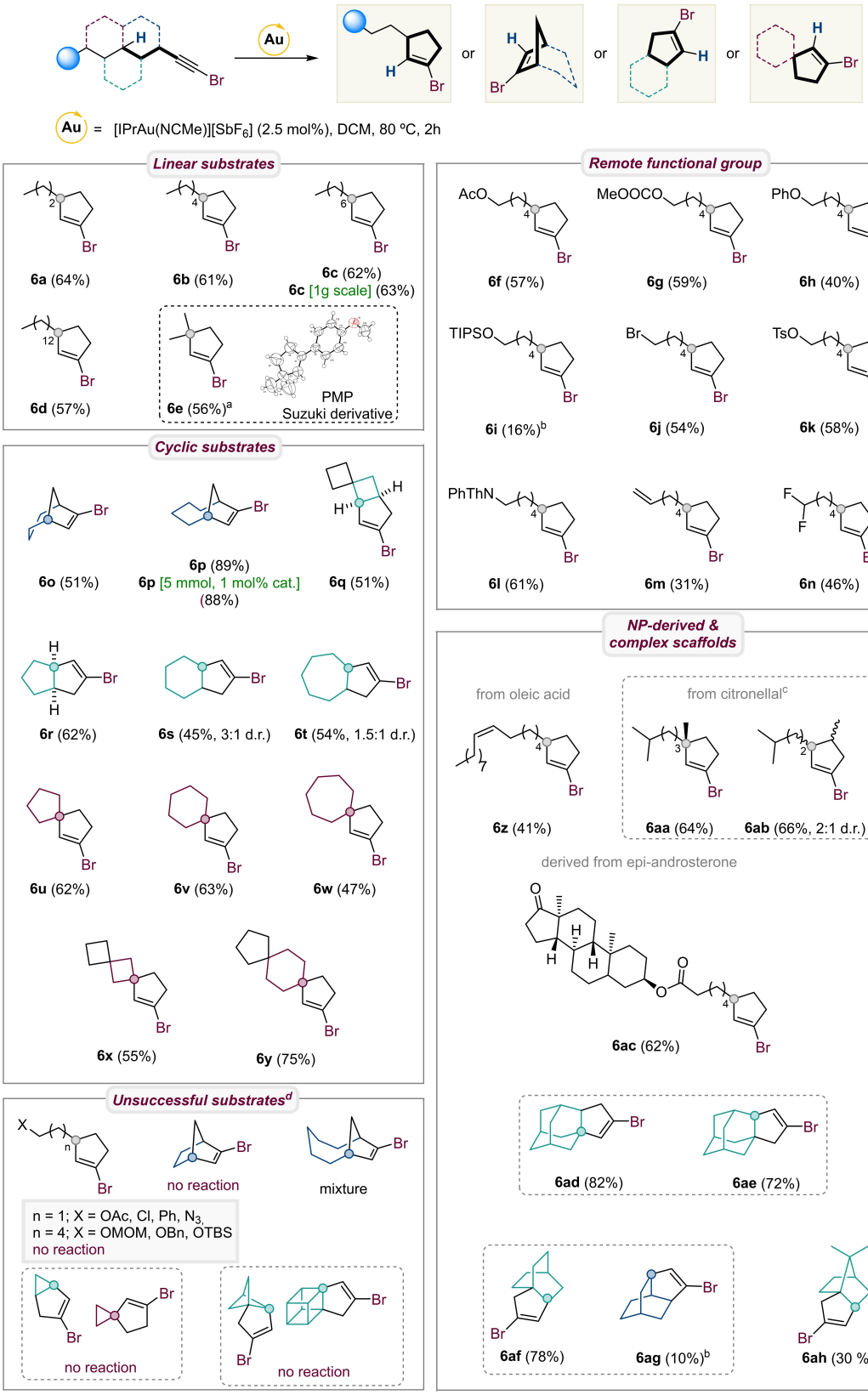

Scheme 1. Scope and limitations. [a] Characterized as a Suzuki derivative due to volatility. [b] NMR yields, characterized from the crude reaction mixtures. [c] From two different derivatives (see SM for details). [d] For a complete list of unsuccessful substrates see Supporting Information (Figure S1).

cyclization affording a biomolecule tethered to the bromocyclopentene core **6ac**. This example would be well-suited for bioconjugation. Finally, some more sophisticated ring systems were synthesized by using polycyclic 1-bromoalkynes as starting material such as the adamantane regioisomeric products **6ad** and **6ae** and the bicyclo[2.2.2]octane derivative **6af**. In this regard, we also observed some limitations when forcing the ring strain. Hence, the bicyclo[2.2.2]octane and bicyclo[2.2.1]heptane derivatives shown in Scheme 1 (NP-derived and complex substrates, **6ag, ah**) only proceeded in poor conversions; whereas the bicyclo[1.1.1]pentane and cubane derivatives did not react at all (Scheme 1, unsuccessful substrates).[23]

Noteworthy, the reaction could be scaled up to 5 mmol (1 g approx.) without compromising its efficiency (Scheme 1, **6c** (63 % vs 62 %) and **6p** (88 % vs 89 %)). Furthermore, by running the reaction at a 5 mmol scale (1 g approx.) the catalyst loading could be diminished to 1 mol% (Scheme 1, **6p**).

As showcased in Scheme 1, the reaction shows great generality concerning the accessible cyclic framework, affording several kinds of mono- and bicyclic scaffolds with well-defined 3D shapes and high sp^3 fraction (Fsp^3) (Figure 2A).[4,21] On the other hand, the selective formation of 5-membered carbocycles is paramount in organic synthesis due to the ubiquitous prevalence of this motif in natural products, pharmaceuticals, and molecules of interest in other industrial fields (Figure 2B). It is worth noting the increasing importance of spirocyclic compounds in medicinal chemistry, and the use of the bicyclo[2.2.2]octane scaffolds as saturated bioisosteres of the phenyl ring.[22a,23b] As shown in Scheme 1, our methodology afforded a varied library of spirocyclic compounds **6u–y** and also one bicyclo[2.2.2]octane derivative **6af**, promising structures for medicinal chemistry.

Derivatizations

The rich chemistry of the $C(sp^2)$–Br bond in the obtained products was then demonstrated by performing several representative transformations (Scheme 2). First, the bromine-lithium exchange reaction allows the introduction of a series of electrophiles at the position initially occupied by the bromine atom. In this way, a formally regioselective deuteration of a double bond (**9**)[24] and the formation of a C10 conjugated enal (**10**) were readily achieved (Scheme 2, a–b). Then several classic palladium-catalyzed cross-coupling reactions (Suzuki, Sonogashira, and Miyaura) allowed the introduction of vinyl (**11**), alkynyl (**12**), and boryl (**13**) appendages, respectively (Scheme 2, c–e). Finally, the oxidation chemistry of the double bond was also put in place, affording synthetically valuable epoxide (**14**) and α-hydroxy ketone (**15**) derivatives, respectively (Scheme 2, f–g).

Principal moments of inertia (PMI) analysis carried out on the herein described library of compounds (parent compounds **6** and derived structures **9–15**) shows a wide spreading throughout the chart by families (see Supporting

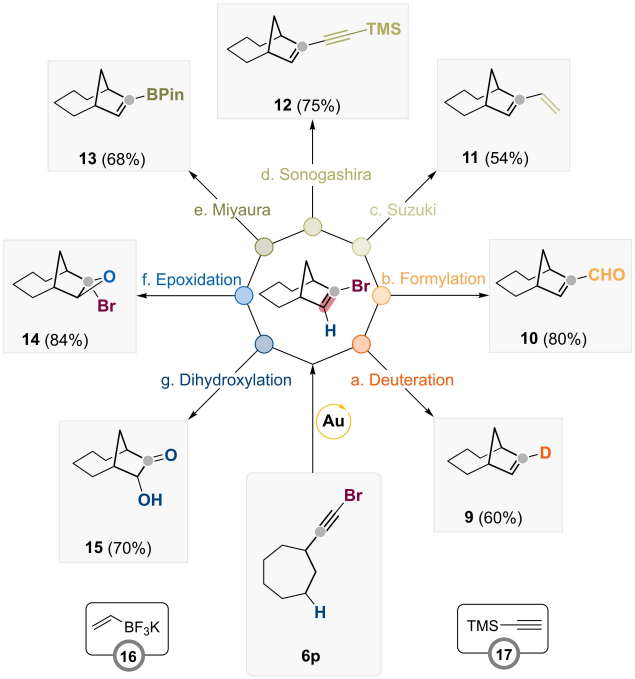

Scheme 2. Derivatizations. Reagents and conditions: a) ^{t}BuLi (2 equiv), THF, −78 °C; then D_2O, −78 °C to r.t. b) ^{t}BuLi (2 equiv), THF, −78 °C; then DMF (1.5 equiv), −78 °C to r.t. c) **16** (1.2 equiv), $Pd(OAc)_2$ (5 mol%), PPh_3 (10 mol%), Cs_2CO_3 (3 equiv), THF:H_2O, 90 °C. d) **17** (1.2 equiv), $dppfPdCl_2$ (2 mol%), CuI (5 mol%), Et_2NH, 30 °C; e) B_2pin_2 (1.1 equiv), $(Ph_3P)_2PdCl_2$ (3 mol%), PPh_3 (6 mol%), PhOK (1.5 equiv); f) *m*-CPBA, CH_2Cl_2:$CHCl_3$ (1 : 1); g) OsO_4 (5 % solution in water, 0,1 mol%), NMO (2,4 equiv), acetone:water:^{t}BuOH (5 : 5 : 1).

Information for details);[25] while products derived from linear substrates show rod-like features (Figure 3, red dots), the bridged bicycle family covers a significant portion of the chart (Figure 3, green dots). The rich chemistry shown in Scheme 2 would allow us to populate the 3D portion of the chart. Noteworthy, a significant number of compounds (ca.

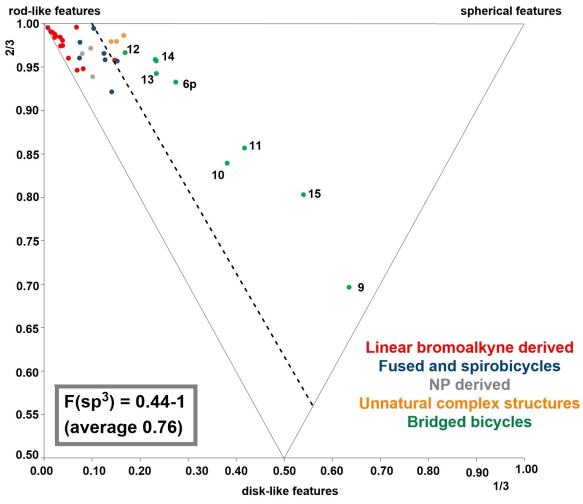

Figure 3. PMI chart.

40 %) deviated from the linear/flat bottom line due to the high Fsp^3 and the intricate molecular skeletons afforded.

Although cyclopentenes are relatively simple skeletons, their synthesis is not always trivial, and the methodology described herein competes well with the existing ones.[26] Even rather simple 3-alkylcyclopentene derivatives are extremely expensive and their synthesis requires several steps.[27] Besides, the selective C(sp^2)–H functionalization might be troublesome (Figure 4). However, the methodology presented herein affords the target derivative in just two simple steps with the added value of obtaining the bromo derivative that renders an immediate entrance to a platform of derivatives, most of them hardly accessible with current methodologies (aldehyde, diene, enyne, boronate…) (Figure 4). Most of the more complex bicyclic derivatives are not commercially available and their synthesis requires expensive and specific substrates (Figure 4).[28] Again, our methodology overwhelms the existing ones allowing the preparation of several kinds of bicyclic derivatives from cheap and readily available starting materials with the added value of easy post-functionalization.

Mechanistic Studies

Based on our results as well as on others, we initially considered the following preliminary mechanism that accounts for the observed connectivity in the final product (Figure 6B, pathway A).[15,20b,29,30] Coordination of the 1-bromoalkyne to the gold center would trigger [1,2]-Br shift, affording the key gold-vinylidene intermediate. Subsequent C–H insertion with exquisite 5 selectivity gives rise to the observed product and regenerates the gold(I) catalyst. A series of experiments were designed to interrogate several features of the proposed mechanism that may support or deny the working hypothesis. To explain the observed connectivity, a ^{13}C-labeled 1-bromoalkyne ^{13}C-**5p** was synthesized and subjected to the optimized reaction conditions (Figure 5A, grey dot). As expected, while the bromine atom is attached to the labeled carbon of the triple bond in the starting material, in the final product the bromine ends up in the non-labeled carbon of the double bond, showcasing the 1,2-[Br] shift (Figure 5A). However, careful monitorization of the reaction by ^{13}C NMR at several temperatures using ^{13}C-**5p** did not allow for observing the intermediacy of any

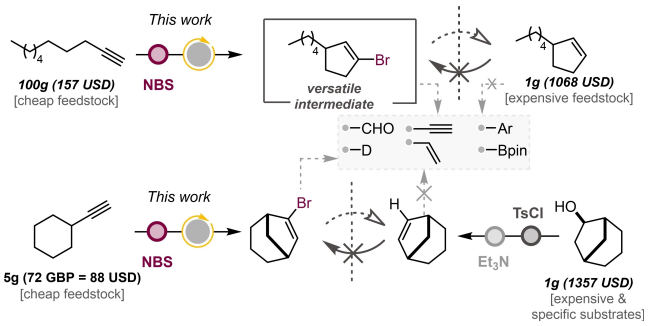

Figure 4. Synthetic relevance.

gold vinylidene intermediate. Above, the stereochemical outcome of the reaction using enantioenriched citronellal derivative (*S*)-**5aa** has already been discussed (see Scheme 1). The lack of racemization observed in this single but conclusive experiment supports a one-step insertion pathway over a two-step [1,5]-H shift/cyclization (Figure 5B). The determination of primary kinetic isotopic effects (pKIE) was carried out by both intra- and intermolecular competition experiments using D-**5c** and D_2-**5c**, respectively (Figure 5C,D).[31] The results obtained both in the inter- and intramolecular competition experiments (KIE = 3.6, and KIE = 2.0, respectively (Figure 5C,D) support C–H insertion being both the substrate-committing and the product-determining step. On the other hand, the measurement of the absolute rates in parallel reactions afforded a KIE value kH/kD = 1, meaning that the C–H insertion is not the turnover-limiting step. Obtaining different values for KIEs measured using these three experimental settings is not uncommon since:[31a] "Using isotopically labeled substrates, site-specific KIEs can be determined using three different approaches: (i) absolute rates, (ii) intermolecular competition, and (iii) intramolecular competition. Crucially, each method entails a different kinetic regime, and for complex reactions may report different KIEs. This is because the three approaches can report the effect that isotopic substitution has on different stages of the reaction pathway. Indeed, great insight can be obtained by comparing KIEs obtained under these three different regimes, and for this reason, they should be considered to be highly complementary. For the same reason, all KIEs should be reported alongside a precise experimental methodology." Another experiment that holds support for this reaction pathway was carried out by using a substrate bearing both a CH and a CH_2 at δ and δ′-positions (Figure 5E). This intramolecular competition experiment showed a preference for the insertion in the CH over the CH_2 as expected for an insertion reaction. To rule out any sort of intermolecular process, labeled compound D_2-**5c** was synthesized and reacted with an equimolecular amount of **5l**. Again, the lack of scrambling observed in this experiment supports the proposed intramolecular process (Figure 5F). Finally, the origin of the reactivity inhibition observed for substrates bearing polar functionalities at distal positions was interrogated. For that aim, a successful non-polar substrate was reacted in the same flask with an unsuccessful polar substrate; the presence of the latter completely inhibited the reactivity of the former, supporting that the origin of such inhibition might be inter- rather than intramolecular (Figure 5G).

To gather further mechanistic evidence, we decided to study the reaction theoretically employing DFT calculations (Figure 6). All the intermediates proposed in our preliminary mechanistic proposal (Figure 7, pathway A), and the corresponding transition states, could be successfully located in the reaction coordinate. However, the theoretical study revealed an unexpected feature: the energy barrier for the C–H insertion step was almost negligible. In agreement with this small energy barrier for this pathway, the calculated KIE for both the inter and the intramolecular competition

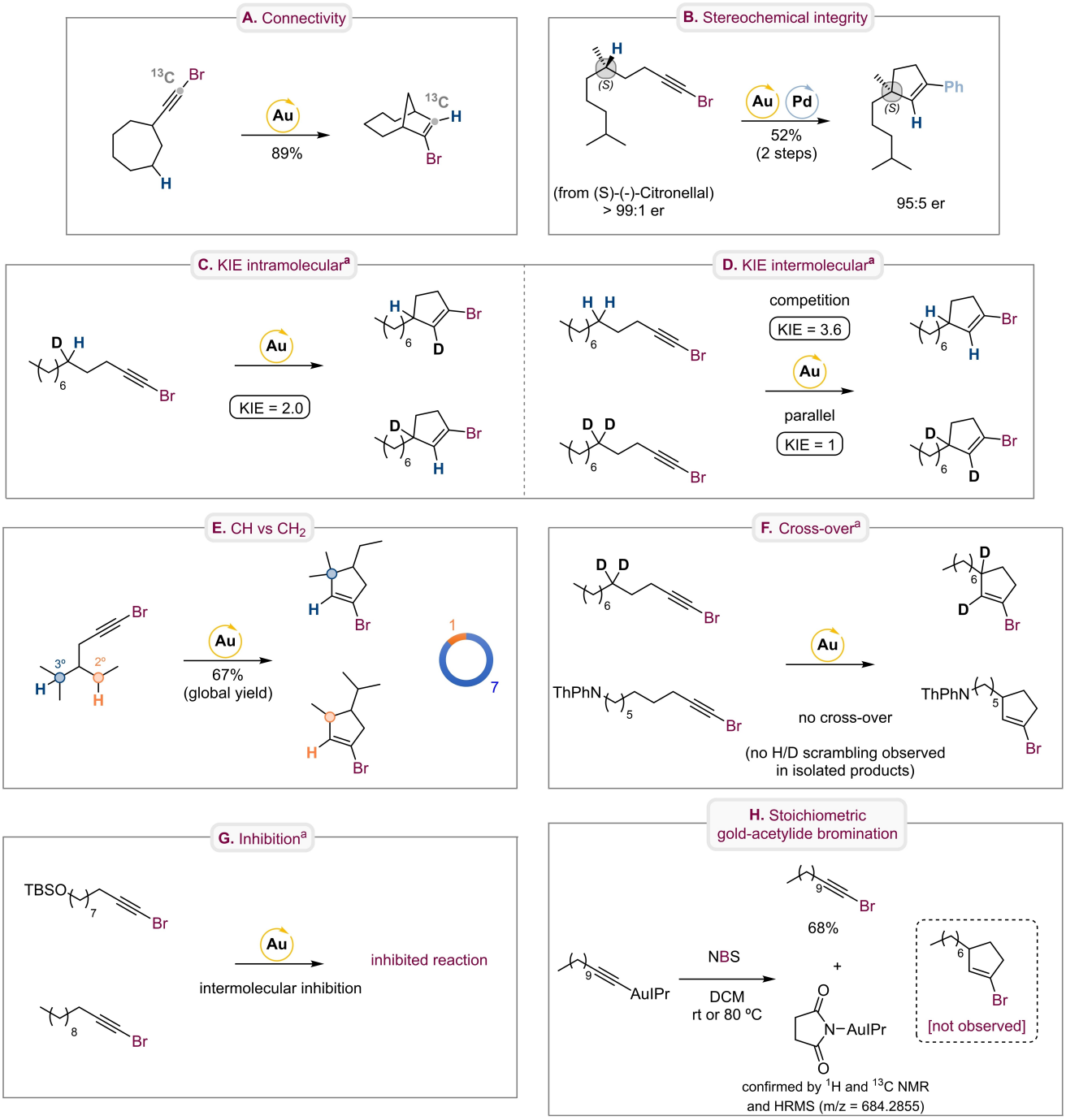

Figure 5. Experimental mechanistic study. [a] Conclusions were drawn from crude NMR spectra and, hence no yields are reported.

experiments is 1 (Figure 6, for details see Supporting Information Figure S7). This unexpected result prompted us to explore alternative mechanistic scenarios. In addition, TS-1 would be analogous to that of the α-bromination of a gold-acetylide complex, already proposed by Zhang (see Figure 1C and reference 16). Aiming to find either further support or disagreement with this reaction pathway, the following stoichiometric experiment was carried out: an isolated IPrAu-acetylide complex was treated with NBS (Figure 5H). Either at room temperature or 80 °C the corresponding bromoalkyne was obtained, meaning that ipso-bromination is preferred over α-bromination, towards vinylidene formation. In comparison, Zhang's intermediate would contain a more nucleophilic α-carbon due to its enolate-like nature. Bringing together our experience with gold-stabilized vinylcarbocations and Gaunt's observations on stereo-retentive C–H insertion of such species,[22b,9] we envisioned an alternative reaction pathway involving concerted C–H insertion of a vinylcation rather than a gold vinylidene key intermediate (Figure 7, pathway B).[32,33] The

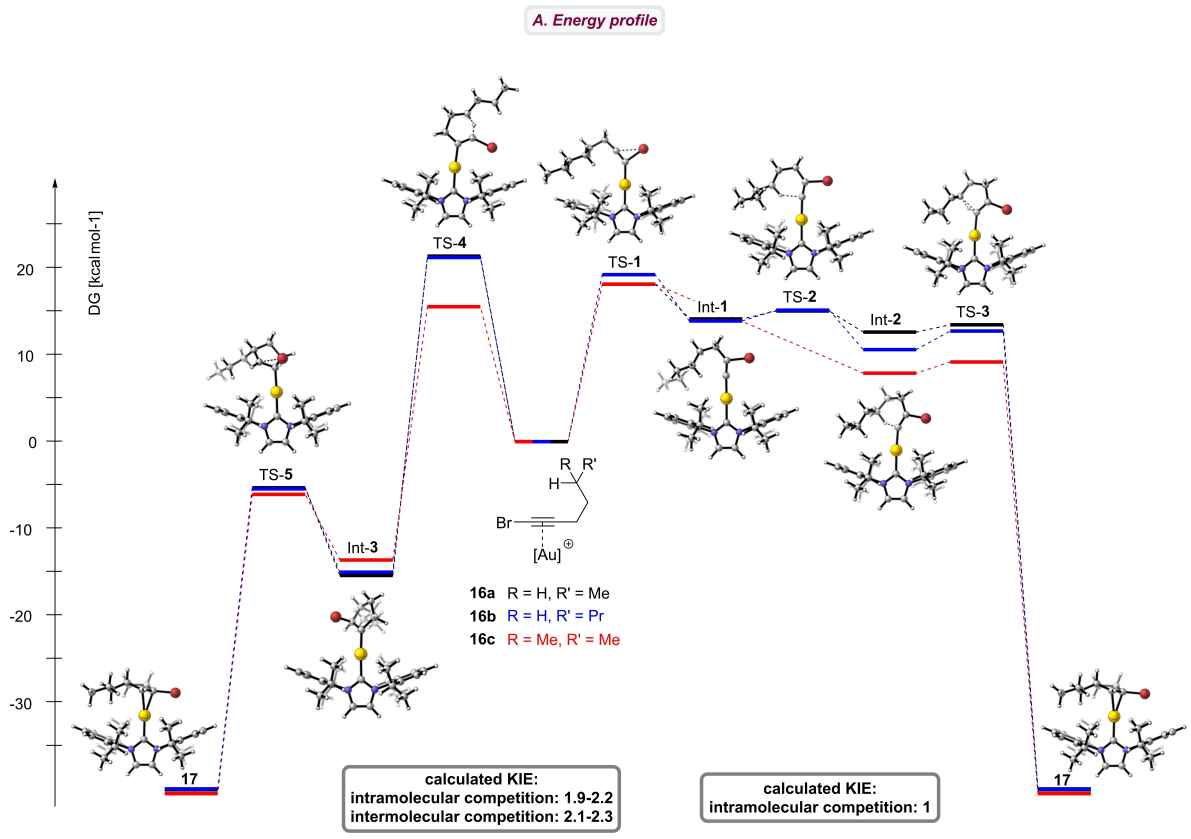

Figure 6. DFT calculations.

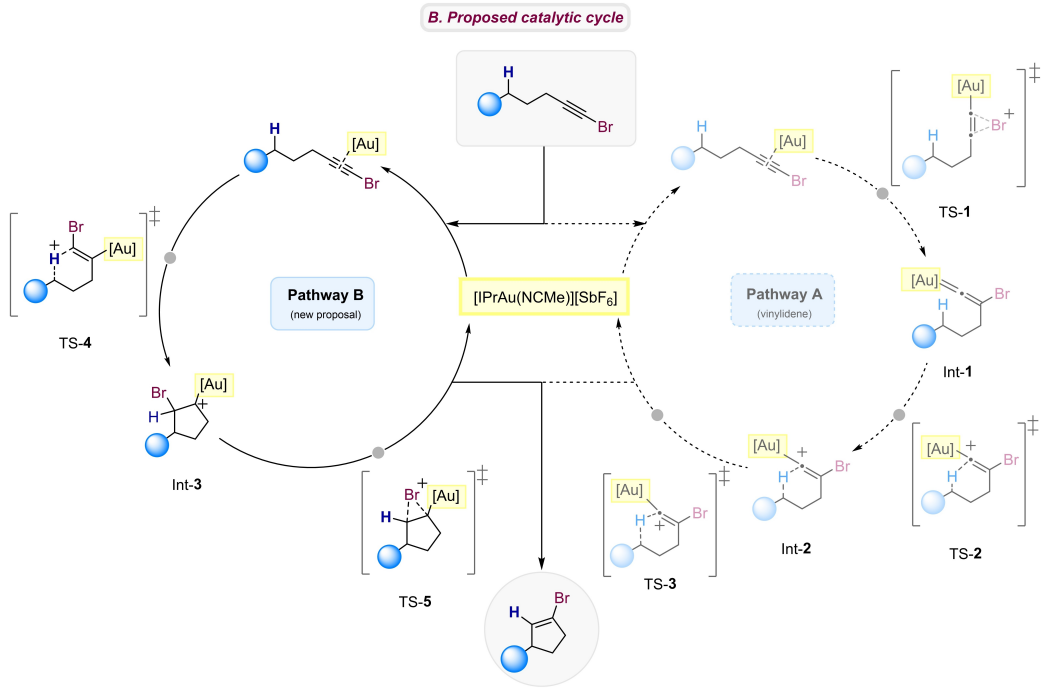

Figure 7. Mechanistic proposal.

corresponding reaction coordinate was calculated, and the results were compatible with the experimental observations. The transition states for both steps (C–H insertion TS-4 and 1,2-Br shift TS-5) were located in the reaction coordinate,

and their geometries and energies were optimized showcasing their viability. Moreover, the calculated KIEs for this reaction pathway match the experimental ones for both the intra- and the intermolecular competition experiments (Figure 6, for details, see Supporting Information Figure S7). To the best of our knowledge, such a reaction pathway has never been described in gold catalysis.[34] In addition, the competing 1,2-H shift was found to proceed via a higher energy transition state, justifying the observed selective 1,2-Br shift (see Supporting Information for details).[35] On the other hand, the pKIE value obtained by the absolute rates of parallel reactions (kH/kD = 1) is in disagreement with the C–H insertion being the turnover limiting step. As judged by the high energy difference between the substrate-gold (**16**) and product-gold (**17**) complexes, we preliminary suggest that the ligand exchange from product to substrate needed for gold to reenter the catalytic cycle might be the turnover limiting step. Moreover, the simultaneous occurrence of both reaction pathways cannot be ruled out as judged by the similar energy of each pathway's highest energy transition state (for full details, see Supporting Information). Further mechanistic studies will be required in order to unambiguously determine the mechanism of this new transformation.

Conclusion

The reaction of aliphatic 1-bromoalkynes under gold catalysis affords the corresponding 1-bromocyclopentene derivatives through a cycloisomerization reaction involving the functionalization of a non-activated C–H bond. A broad set of mono- and bicycles has been obtained affording an assorted library of diverse scaffolds under extremely simple reaction conditions. The presence of a readily functionalizable C(sp^2)–Br bond in the products allowed us to increase the molecular diversity amenable to our methodology. A preliminary mechanistic study supports a concerted C–H bond breaking/C–C bond forming pathway in agreement with the experimental and computational data. Further studies aimed at applying this transformation to the synthesis of complex molecules and libraries of compounds as well as at studying its mechanism in-depth are currently underway in our laboratories.

Acknowledgements

JM and PB gratefully acknowledge the Spanish Agencia Estatal de Investigación (AEI) for a grant (PID2019-107469RB-I00) and a Ramón y Cajal contract (RyC-2016-20951), respectively. NS and GH thank the Deutsche Forschungsgemeinschaft for a grant (HA 2973/17-1). Marta Arimont and Dr. Natalia Mateu from Pharmenable are gratefully acknowledged for the execution and help with the interpretation of the PMI chart. Prof. Guy Lloyd-Jones is gratefully acknowledged for helpful discussion on NMR-based methods for the determination of KIEs. Prof. Alfredo Ballesteros and Prof. Félix Rodríguez are acknowledged for helpful discussions. Prof. Rubén Martín and Prof. Rubén Vicente are acknowledged for proofreading the manuscript.

Conflict of Interest

The authors declare no conflict of interest.

Data Availability Statement

The data that support the findings of this study are available in the supplementary material of this article.

Keywords: C–H Bond Activation · DFT Calculations · Gold Catalysis · Molecular Diversity · Vinyl Cation

[1] For selected reviews on C–H bond functionalization, see: a) T. W. Lyons, M. S. Sanford, *Chem. Rev.* **2010**, *110*, 1147–1169; b) L. Ackermann, *Chem. Rev.* **2011**, *111*, 1315–1345; c) O. Daugulis, J. Roane, L. D. Tran, *Acc. Chem. Res.* **2015**, *48*, 1053–1064; d) J. He, M. Wasa, K. S. L. Chan, Q. Shao, J.-Q. Yu, *Chem. Rev.* **2017**, *117*, 8754–8786; e) N. Y. S. Lam, K. Wu, J.-Q. Yu, *Angew. Chem. Int. Ed.* **2021**, *60*, 15767–15790.

[2] For selected recent examples of C–H activation on biased substrates, see: a) L. C. Greiner, N. Arichi, S. Inuki, H. Ohno, *Angew. Chem. Int. Ed.* **2023**, *62*, e202213653; b) D. F. León Rayo, A. Mansour, W. Wu, B. N. Bhawal, F. Gagosz, *Angew. Chem. Int. Ed.* **2023**, *62*, e202212893; c) Z. Liu, H. P. Wang, S. P. Nolan, Q. Song, W. Yu, X. Jiang, E. A. Anderson, X. Bi, *Nat. Commun.* **2022**, *13*, 1674; d) Y. T. Boni, R. C. Cammarota, K. Liao, M. S. Sigman, H. M. L. Davies, *J. Am. Chem. Soc.* **2022**, *144*, 15549–15561; e) R. C. Cammarota, W. Liu, J. Bacsa, H. M. L. Davies, M. S. Sigman, *J. Am. Chem. Soc.* **2022**, *144*, 1881–1898; f) Y.-W. Chen, Y. Liu, H.-Y. Lu, G.-Q. Lin, Z.-T. He, *Nat. Commun.* **2021**, *12*, 5626; g) T. C. Wang, L. Zhu, S. Luo, Z.-S. Nong, P.-S. Wang, L.-Z. Gong, *J. Am. Chem. Soc.* **2021**, *143*, 20454–20461.

[3] For pioneering examples on the use of directing groups for C(sp^3)–H activation, see: a) N. Chatani, T. Asaumi, T. Ikeda, S. Yorimitsu, Y. Ishii, F. Kakiuchi, S. Murai, *J. Am. Chem. Soc.* **2000**, *122*, 12882–12883; b) L. V. Desai, K. L. Hull, M. S. Sanford, *J. Am. Chem. Soc.* **2004**, *126*, 9542; c) V. G. Zaitsev, D. Shabashov, O. Daugulis, *J. Am. Chem. Soc.* **2005**, *127*, 13154–13155; d) R. Giri, X. Chen, J.-Q. Yu, *Angew. Chem. Int. Ed.* **2005**, *44*, 2112–2115; e) B. V. S. Reddy, L. R. Reddy, E. J. Corey, *Org. Lett.* **2006**, *8*, 3391–3394.

[4] F. Lovering, *MedChemComm* **2013**, *4*, 515–519.

[5] G. Klebe, F. Dullweber, H.-J. Böhm, *Thermodynamic models of Drug-Receptor Interactions: a General Introduction in Drug-Receptor Thermodynamics: Introduction and Applications* (Ed. Robert B. Raffa), Wiley, Chichester, New York, **2001**, pp. 83–104.

[6] For a recent review, see: a) W. Guo, Q. Wang, J. Zhu, *Chem. Soc. Rev.* **2021**, *50*, 7359–7377. b) For selected recent examples, see:N. Li, J. Li, M. Qin, J. Li, J. Han, C. Zhu, W. Li, J. Xie, *Nat. Commun.* **2022**, *13*, 4224; c) S. Munnuri, J. R. Falck, *J. Am. Chem. Soc.* **2022**, *144*, 17989–17998; d) K. M. Nakafuku, Z. Zhang, E. A. Wappes, L. M. Stateman, A. D. Chen, D. A. Nagib, *Nat. Chem.* **2020**, *12*, 697–704.

[7] For a recent example, see: Y. Zhou, Y. Qin, Q. Wang, Z. Zhang, G. Zhu, *Angew. Chem. Int. Ed.* **2022**, *61*, e202110864.

[8] G. A. Olah, *J. Org. Chem.* **2001**, *66*, 5943–5957.

[9] F. Zhang, S. Das, A. J. Walkinshaw, A. Casitas, M. Taylor, M. G. Suero, M. J. Gaunt, *J. Am. Chem. Soc.* **2014**, *136*, 8851–8854.
[10] S. Popov, B. Shao, A. L. Bagdasarian, T. R. Benton, L. Zou, Z. Yang, K. N. Houk, H. M. Nelson, *Science* **2018**, *361*, 381–387.
[11] For a pioneering report of a free carbene species, see: W. R. Moore, H. R. Ward, R. F. Merritt, *J. Am. Chem. Soc.* **1961**, *83*, 2019–2020.
[12] For an excellent review on metal-carbene insertion reactions, see: M. P. Doyle, R. Duffy, M. Ratnikov, L. Zhou, *Chem. Rev.* **2010**, *110*, 704–724.
[13] M. Karpf, A. S. Dreiding, *Helv. Chim. Acta* **1979**, *62*, 852.
[14] B. L. Williamson, R. R. Tykwinski, P. J. Stang, *J. Am. Chem. Soc.* **1994**, *116*, 93.
[15] P. Morán-Poladura, E. Rubio, J. M. González, *Angew. Chem. Int. Ed.* **2015**, *54*, 3052–3055.
[16] Y. Wang, M. Zarca, L.-Z. Gong, L. Zhang, *J. Am. Chem. Soc.* **2016**, *138*, 7516–7519.
[17] For reviews covering gold vinylidene chemistry, see: a) F. Gagosz, *Synthesis* **2019**, *51*, 1087–1099; b) X. Zhao, M. Rudolph, A. S. K. Hashmi, *Chem. Commun.* **2019**, *55*, 12127–12135; c) A. S. K. Hashmi, *Acc. Chem. Res.* **2014**, *47*, 3, 864–876; d) I. Braun, A. M. Asiri, A. S. K. Hashmi, *ACS Catal.* **2013**, *3*, 1902–1907. e) For seminal contributions, see:A. S. K. Hashmi, I. Braun, M. Rudolph, F. Rominger, *Organometallics* **2012**, *31*, 644–661; f) V. Mamane, P. Hannen, A. Fürstner, *Chem. Eur. J.* **2004**, *10*, 4556–4575. For a recent report, see: g) D. F. León Rayo, Y. J. Hong, D. Campeau, D. J. Tantillo, F. Gagosz, *Chem. Eur. J.* **2021**, *27*, 10637–10648.
[18] For examples of gold-vinylidene insertion into conformationally biased C–H bonds, see: a) P. Nösel, L. N. dos Santos Comprido, T. Lauterbach, M. Rudolph, F. Rominger, A. S. K. Hashmi, *J. Am. Chem. Soc.* **2013**, *135*, 15662–15666; b) L. Ye, Y. Wang, D. H. Aue, L. Zhang, *J. Am. Chem. Soc.* **2012**, *134*, 31–34. c) For examples of gold-carbene insertions into conformationally biased C–H bonds, see:J. Barluenga, R. Sigüeiro, R. Vicente, A. Ballesteros, M. Tomás, M. A. Rodríguez, *Angew. Chem. Int. Ed.* **2012**, *51*, 10377–10381; d) Y. Horino, T. Yamamoto, K. Ueda, S. Kuroda, F. D. Toste, *J. Am. Chem. Soc.* **2009**, *131*, 2809–2811.
[19] For a recent review on gold-catalyzed C–H activation, see: G. Meera, K. R. Rohit, G. S. S. Treesa, G. Anilkumar, *Asian J. Org. Chem.* **2020**, *9*, 144–161.
[20] a) P. D. García-Fernández, J. Iglesias-Sigüenza, P. S. Rivero-Jerez, E. Díez, E. Gómez-Bengoa, R. Fernández, J. M. Lassaletta, *J. Am. Chem. Soc.* **2020**, *142*, 16082–16089; b) M. Kreuzahler, A. Daniels, C. Wölper, G. Haberhauer, *J. Am. Chem. Soc.* **2019**, *141*, 1337–1348; c) M–E. de Orbe, M. Zanini, O. Quinonero, A. Echavarren, *ACS Catal.* **2019**, *9*, 7817–7822. d) Under certain reaction conditions, 1-haloalkynes have been reported to undergo oxidative addition with gold (I) species, see:Y. Yang, J. Schießl, S. Zallouz, V. Göker, J. Gross, M. Rudolph, F. Rominger, A. S. K. Hashmi, *Chem. Eur. J.* **2019**, *25*, 9624–9628.
[21] a) M. Garcia-Castro, S. Zimmermann, M. G. Sankar, K. Kumar, *Angew. Chem. Int. Ed.* **2016**, *55*, 7586–7605; b) F. Lovering, J. Bikker, C. Humblet, *J. Med. Chem.* **2009**, *52*, 6752–6756.
[22] a) K. Hiesinger, D. Dar'in, E. Proschak, M. Krasavin, *J. Med. Chem.* **2021**, *64*, 150–183; b) V. A. D'yakonov, O. A. Trapeznikova, A. de Meijere, U. M. Dzhemilev, *Chem. Rev.* **2014**, *114*, 5775–5814.
[23] a) For a report showing the inertness of propellane derivatives in intramolecular C–H activation, see: R. M. Bychek, V. Hutskalova, Y. P. Bas, O. A. Zaporozhets, S. Zozulya, V. V. Levterov, P. K. Mykhailiuk, *J. Org. Chem.* **2019**, *84*, 15106–15117. b) For a recent review on saturated bioisosteres of the phenyl ring highlighting the role of the bicyclo[111]pentane, bicyclo[222]octane, and cubane scaffolds, see:P. K. Mykhailiuk, *Org. Biomol. Chem.* **2019**, *17*, 2839–2849.
[24] T. Pirali, M. Serafini, S. Cargnin, A. A. Genazzani, *J. Med. Chem.* **2019**, *62*, 5276–5297.
[25] W. H. B. Sauer, M. K. Schwarz, *J. Chem. Inf. Comput. Sci.* **2003**, *43*, 987–1003.
[26] a) H. R. Rounds, M. Zeller, C. Uyeda, *Organometallics* **2018**, *37*, 545–550; b) H. You, E. Rideau, M. Sider, S. P. Fletcher, *Nature* **2015**, *517*, 351–355; c) N. Suzuki, D. Y. Kondakov, T. Takahashi, *J. Am. Chem. Soc.* **1993**, *115*, 8485–8486; d) J. K. Crandall, A. C. Clark, *Tetrahedron Lett.* **1969**, *10*, 325–328.
[27] The prices depicted in Figure 4 correspond to the cheapest ones found in a SciFinder search (16/01/2023).
[28] C. A. Grob, U. Zutter, *Tetrahedron Lett.* **1982**, *23*, 2849–2852.
[29] Y. Xia, A. S. Dudnik, Y. Li, V. Gevorgyan, *Org. Lett.* **2010**, *12*, 5538–5541.
[30] J. Bucher, T. Wurm, K. S. Nalivela, M. Rudolph, F. Rominger, A. S. K. Hashmi, *Angew. Chem. Int. Ed.* **2014**, *53*, 3854–3858.
[31] a) Y. Ben-Tal, P. J. Boaler, H. J. A. Dale, R. E. Dooley, N. A. Fohn, Y. Gao, A. García-Domínguez, K. M. Grant, A. M. R. Hall, H. L. D. Hayes, M. M. Kucharski, R. Wei, G. C. Lloyd-Jones, *Prog. Nucl. Magn. Reson. Spectrosc.* **2022**, *129*, 28–106; b) E. M. Simmons, J. F. Hartwig, *Angew. Chem. Int. Ed.* **2012**, *51*, 3066–3072.
[32] The bonding in gold ylidene complexes has been studied in-depth by Klein and Hashmi, see: a) D. Sorbelli, L. Nunes dos Santos Comprido, G. Knizia, A. S. K. Hashmi, L. Belpassi, P. Belanzoni, J. E. M. N. Klein, *ChemPhysChem* **2019**, *20*, 1671–1679; b) J. E. M. N. Klein, G. Knizia, L. Nunes dos Santos Comprido, J. Kästner, A. S. K. Hashmi, *Chem. Eur. J.* **2017**, *23*, 16097–16103; c) L. Nunes dos Santos Comprido, J. E. M. N. Klein, G. Knizia, J. Kästner, A. S. K. Hashmi, *Chem. Eur. J.* **2016**, *22*, 2892–2895; d) M. Wieteck, Y. Tokimizu, M. Rudolph, F. Rominger, H. Ohno, N. Fujii, A. S. K. Hashmi, *Chem. Eur. J.* **2014**, *20*, 16331–16336; e) A. S. K. Hashmi, M. Wieteck, I. Braun, M. Rudolph, F. Rominger, *Angew. Chem. Int. Ed.* **2012**, *51*, 10633–10637.
[33] For reviews on intermediates in gold catalysis, see: a) T. Lauterbach, A. M. Asiri, A. S. K. Hashmi, *Adv. Organomet. Chem.* **2014**, *62*, 261–297; b) A. S. K. Hashmi, *Angew. Chem. Int. Ed.* **2010**, *49*, 5232–5241.
[34] In a different context, the C—H insertion of a partially related vinylcation under gold catalysis has been reported by Yu: a) Y. Wang, P.-J. Cai, Z.-X. Yu, *J. Am. Chem. Soc.* **2020**, *142*, 2777 – 2786. b) P.-J. Cai, Y. Wang, C.-H. Liu, Z.-X. Yu, *Org. Lett.* **2014**, *16*, 5898 – 5901.
[35] For similar findings, see: a) W. Guo, Y. Xia, *Synthesis* **2014**, *46*, 2149–2154; b) A. W. Sromek, M. Rubina, V. Gevorgyan, *J. Am. Chem. Soc.* **2005**, *127*, 10500–10501.
[36] Deposition number 2168679 (for **6e′**) contains the supplementary crystallographic data for this paper. These data are provided free of charge by the joint Cambridge Crystallographic Data Centre and Fachinformationszentrum Karlsruhe Access Structures service.

Manuscript received: April 14, 2023
Accepted manuscript online: April 27, 2023
Version of record online: May 12, 2023